sustainability

MDPI

Article

Numerical Study on the Behavior of an Existing Tunnel during Excavating Adjacent Deep Foundation Pit

Jianwei Liu [1], Bingshuang Xue [1], Haibo Wang [1], Xuemin Zhang [2] and Yongxing Zhang [1,*]

1 School of Civil Engineering, Nanjing Forestry University, Nanjing 210037, China
2 School of Civil Engineering, Central South University, Changsha 410075, China
* Correspondence: zhanguongxing81@aliyun.com

Abstract: The excavation of a deep foundation pit adjacent to an existing tunnel may lead to the large deformation and induce damages in the tunnel structure. However, the influence on existing tunnel structure from nearby excavations has not been understood clearly, since it is affected by complex influencing factors of not only the geological and topographical conditions but also the construction method and positional relationship of the adjacent structures. This paper presents a numerical investigation into an existing underground rail transit line during the excavation of an adjacent deep foundation pit, in which the behavior of the existing tunnel structure from excavating the aforementioned foundation pit is clarified, and the effectiveness of the adopted three-dimensional model is confirmed by comparison between the numerically calculated and field-measured ground settlement of the monitoring point. The results demonstrate that the deformation of the existing tunnel structure is mostly induced by the excavation of the deep foundation pit. This study can provide a reference of deep excavations adjacent to existing infrastructures.

Keywords: behavior influence; structure safety; adjacent existing tunnel; foundation pit excavation; numerical investigation

Citation: Liu, J.; Xue, B.; Wang, H.; Zhang, X.; Zhang, Y. Numerical Study on the Behavior of an Existing Tunnel during Excavating Adjacent Deep Foundation Pit. *Sustainability* **2023**, *15*, 9740. https://doi.org/10.3390/su15129740

Academic Editors: Jun Hu, Guan Chen and Yong Fu

Received: 23 May 2023
Revised: 13 June 2023
Accepted: 16 June 2023
Published: 19 June 2023

1. Introduction

Urban railway transportation systems have been widely developed and utilized with the acceleration of urbanization in China. However, there are still many problems and challenges of constructing underground engineering, in which many foundation pits are inevitably adjacent to existing tunnel lines. The clear distance between the foundation pit and the existing tunnel lines is becoming smaller, may be even less than 1 m [1]. The relationship between the foundation pits of new engineering and adjacent existing tunnels is becoming more and more complex, as the excavation of new foundation pits may change the stress state of the surrounding soil not only by the disturbance of surrounding soil but also by the reduction in underground water, causing large deformations to the existing nearby tunnels through uneven settlement [2]. Severe damage through segment cracking, leakage and even longitudinal distortion of railway tracks may likely occur when the tunnel deformation and internal forces exceed the capacity of tunnel structures [3,4]. Therefore, it is important to study the influence on and ensure the safety of the existing tunnel lines from excavating the adjacent foundation pits, by controlling the deformation of tunnel structures and the settlement of the ground surface.

In recent years, much research has focused on the behavior of existing tunnel structure during adjacent excavations by theoretical analysis, field monitoring, and numerical simulation. In theoretical analysis and numerical simulation, analytical models using Mindlin's displacement solutions and fuzzy mathematics theory have been developed for the theoretical and numerical analysis of tunnel deformation creating optimized procedures for constructing foundation pits, and practical engineering has verified the effectiveness and success of this method [5,6]. Moreover, two-stage analysis methods have been proposed for rationally simplifying the additional loads acting on the existing tunnel and introducing the existing tunnel as an elastic beam on a Pasternak foundation [7–9], in which case the modified subgrade coefficient is employed in the Pasternak foundation [10,11]. These theoretical and numerical methods are used to evaluate the disturbance effect of surrounding soil, model the collapse process of the deep foundation pit, and determine the deformation behavior of the existing tunnel as well as analyzing the influencing factors of the tunnel deformation caused by the excavation of the adjacent foundation pit [12–14].

Field monitoring is generally implemented alongside numerical simulation [15]. In previous studies, the three-dimensional finite difference method in combination with on-site test data is employed to analyze the deformation and stability of existing tunnel structure as well as predict weak areas during excavating the adjacent deep foundation pit [16–18]. The finite element method combined with on-site monitoring is utilized to analyze the law of stress and deformation in the process of deep foundation pit excavation [19]. There are many case studies of the performance variation of different infrastructures during excavating adjacent foundation pits, and reasonable strengthening measures are studied and proposed. The reinforcement mechanisms and reinforcement depths of surrounding soil that may influence tunnel deformation and uplift are studied with respect to controlled stress relief [20]. The response of six existing buildings from excavating the deep foundation pit of a subway station has been numerically investigated, in which the proposed method of modifying the lateral deflection of the retaining wall to reduce ground settlement proved a more cost-effective alternative [21].

There are many studies on the behavior of existing tunnels and foundation pit supporting structures. However, the behavior of the tunnel structure induced by excavating an adjacent foundation pit have not been understood clearly, since it is affected by complex influencing factors of not only geological and topographical conditions but also the construction method and positional relationship of the adjacent structures. Therefore, further study is required on the influence of existing tunnels from excavating adjacent foundation pits, which is expected to provide a basis for rationally adopting protective measures in excavating the foundation pit. In this paper, a case study is presented of the investigation using numerical simulation into the existing rail transit line 7 during excavating an adjacent deep foundation pit, in which the deformation of tunnel structure and stresses of underground continuous wall are studied, and the effectiveness of the adopted three-dimensional numerical model is validated by comparison between the numerical results and field measures.

2. Engineering Background

2.1. Engineering Profile

A deep foundation pit was excavated to build the Fumin Station of rail transit line 10, which is adjacent to the existing left-line and right-line tunnels in rail transit line 7. The thickness of the covering soil ranged from 5.15 m to 5.61 m, the width of the foundation pit ranged from 21.9 m to 27.9 m, with a width of 21.9 m in the standard section, and the depth of the foundation pit ranged from 19.26 m to 21.64 m, in which the shield launching shaft of 27.9 m width and 21.5 m excavation depth was set at the south end of the station. The outer edge of rail transit line 7 is only 7.85 m away from the foundation pit at the south end of Fumin Station. The project plan and the positional relationship between the tunnel and foundation pit are shown in Figures 1 and 2, respectively.

2.2. Hydrogeological Conditions

The foundation pit of Fumin Station in the project mainly crossed the complex soil layers from top to bottom, including plain soil, silty clay soil, round gravel, sand-like strongly weathered granite, moderately weathered granite, and slightly weathered granite. There were two main types of groundwater around the station: loose rock pore water and bedrock fracture water, which are mainly found in the strongly weathered block and moderately weathered zone with slight compression. There was no differential weathering of the strata during the survey process, that would result in the formation of solitary stones or weathered deep grooves with soft and hard layers, and the ground surface water was not abundant and mainly consisted of accumulated water in potholes. After the excavation of soil slopes formed by residual granite soil and completely weathered rock, the unloading action caused the soil on the free surface to easily slide along the primary or secondary structural planes due to the geotechnical characteristics of the granite formation, and it was prone to collapse due to the residual soil of granite and completely weathered rock being soaked in water, since there was a very long rainy season around the construction period. Moreover, river water was drained during the processes of excavation and reinforcement of the deep foundation pit, which was expected to ensure the safety of the deep foundation pit slope and surrounding environment.

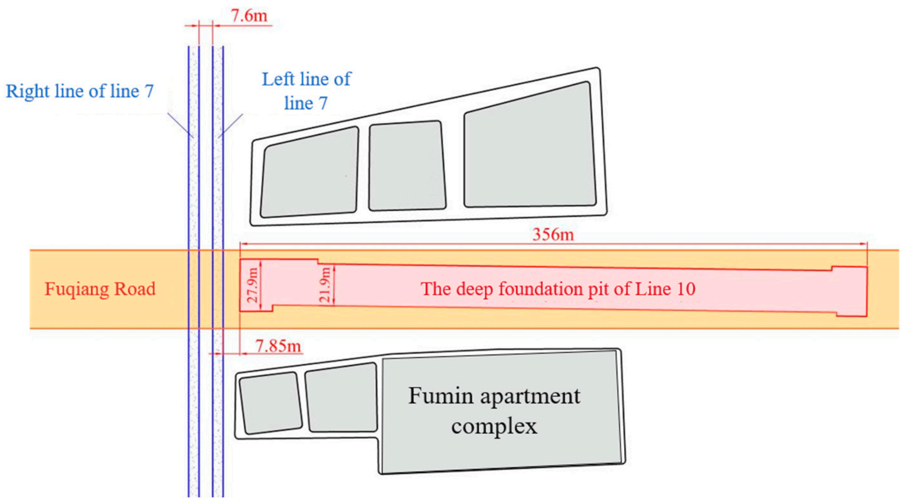

Figure 1. Plan of the project.

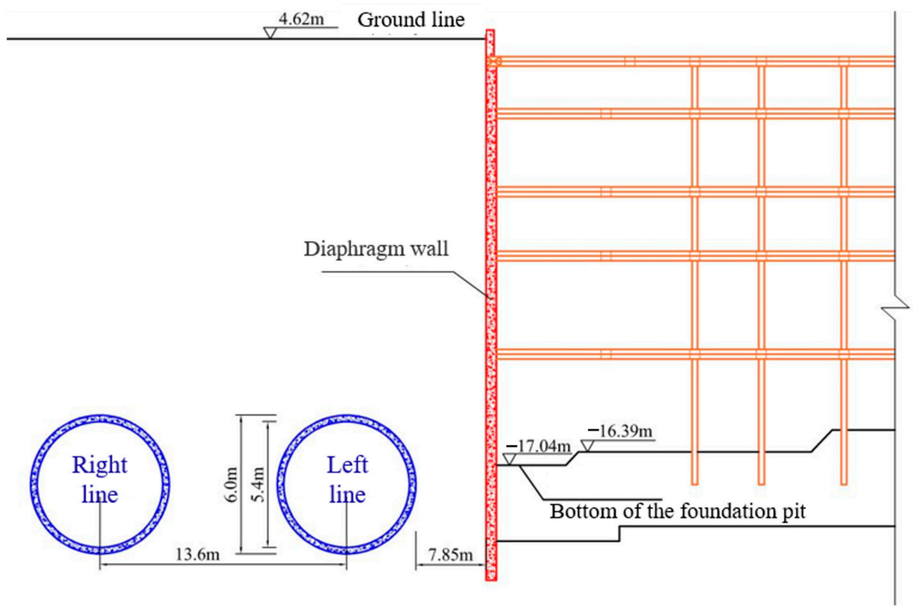

Figure 2. Profile of the existing tunnel and the foundation pit.

2.3. Reinforcement Measure outside the Foundation Pit

Reinforcement measures in the passive zone were used to reinforce the deep foundation pit for safe excavation, and the specific reinforcement measures are shown in Figure 3, in which the labels A, B and D are the width, length and depth of the reinforcement zone, respectively, and label C is the elastic modulus of the reinforced soil surrounding the deep foundation pit.

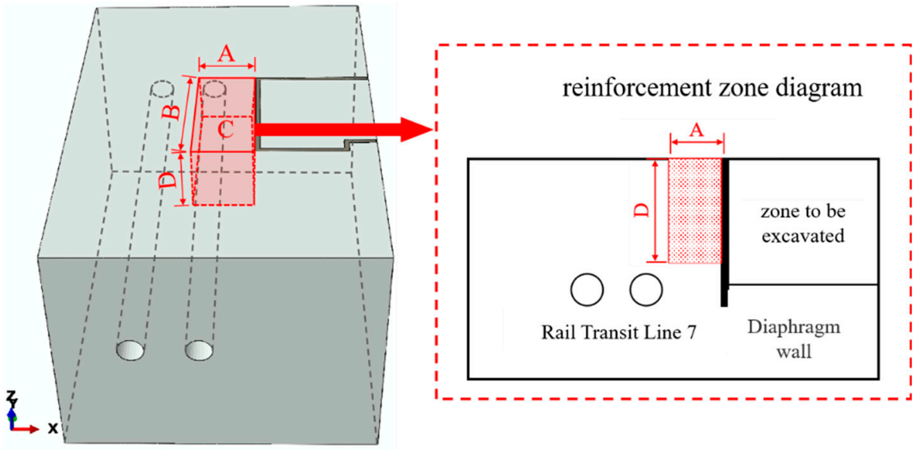

Figure 3. Reinforcement zone diagram.

The foundation pit was excavated in six layers, in which the depths of the excavated layers were −1.8 m, −4.7 m, −8.7 m, −12 m, −17 m and −21.5 m, respectively. Moreover, the support structures were constructed with the excavation of every layer.

3. Proposal and Validation of the Numerical Investigation Model

3.1. Three-Dimensional Numerical Model and Material Properties

Figure 4 shows the three-dimensional numerical model used to calculate the deformation and internal force of the tunnel structure while excavating the adjacent deep foundation pit, in which the numerical model sets each layer as horizontal due to the relatively small ground fluctuation at the construction site. Moreover, the deep foundation pit of Fumin Station, the double-line shield tunnel of the existing rail transit line 7 and the surrounding soil are included in the numerical model, in which the excavation area of the foundation pit is within a range of 50 m near the operation area of the existing rail transit line 7.

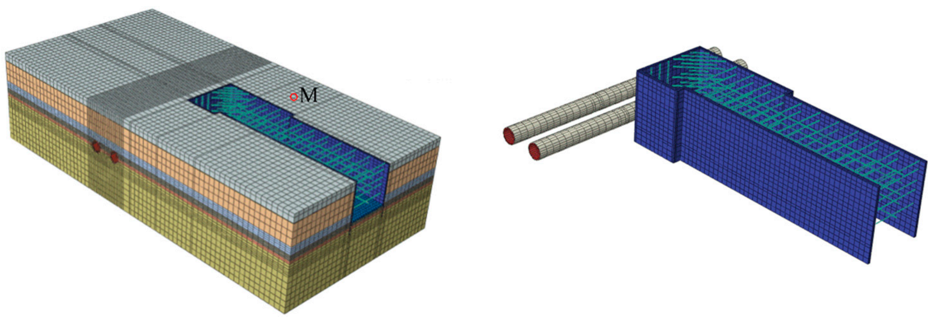

Figure 4. Three-dimensional model of numerical calculation.

The size of the entire model is about three times that of the excavated foundation pit, in which the calculated ranges in longitudinal, vertical and side directions are 200 m, 50 m and 100 m, respectively. There are some assumptions regarding the boundary conditions of the numerical model: the four sides are horizontally constrained, the bottom is horizontally and vertically constrained, and the upper boundary is a free boundary. The hexahedral reduced integral element is used for simulating surrounding rocks, shield tunnel segments and the underground continuous wall, and the two-nodes spatial linear beam element is used for simulating the concrete supporting system. In the model, the connection of surrounding rocks and grouting layer, grouting layer and shield tunnel segment, underground continuous wall, and concrete supporting system are simulated using a binding constraint, and the surface-to-surface contact with normal hard contact and tangential friction is set between the underground continuous wall and surrounding rocks. In the numerical simulation, the existing rail transit line 7 is constructed first due to the actual construction time sequence, and the balance of crustal stress is carried out after the construction is completed to avoid the interference on the operation area of the existing rail transit line 7.

The numerical model is meshed using structural and scanning techniques in Midas FE software as shown in Figure 4, in which the soil contains 101,127 elements and 109,320 nodes, the underground continuous wall contains 4284 elements and 6858 nodes, and the concrete supporting system with five total layers contains 409 elements and 416 nodes. Moreover, the influence of excavating the deep foundation pit adjacent to the operation area of the existing rail transit line 7 is considered, in which the stress release process of the surrounding soil for the shield tunnel in rail transit line 7 is simulated using the softening modulus method, and the hardening of the grouting layer is simulated employing the changes of temperature field stress. The excavation and supporting of the foundation pit are implemented using activating and killing elements in the numerical simulation. The foundation pit is also excavated with six layers in the numerical simulation, and the excavation depths of the excavated layers also are −1.8 m, −4.7 m, −8.7 m, −12 m, −17 m and −21.5 m, respectively, corresponding to field observations.

The three-dimensional numerical model sets every layer as horizontal and assumes that every layer of the surrounding soils has homogeneous material properties in the numerical analysis. The surrounding soil is considered as ideal elastic-plastic material with a Mohr–Coulomb yield criterion in the numerical simulation [22], and the main parameters of surrounding rocks are shown in Table 1.

Table 1. Parameters of surrounding rocks.

Soil Layer	Depth	Unit Weight	Elastic Modulus	Poisson's Ratio	Cohesive Force	Friction Angle
	m	kg/m^3	MPa		kPa	°
plain soil	4.5	1790	6	0.4	10	10
silty clay soil	11.5	1730	6	0.43	14	10
round gravel	4	2000	28	0.25	0	30
strongly weathered granite	3	2050	96	0.22	35	28
moderately weathered granite	1.5	2530	500	0.22	3000	38
slightly weathered granite	25.5	2610	5000	0.22	6000	52

3.2. Numerical Model Validation

To verify the reliability of the adopted three-dimensional numerical model, the simulated calculation values are selected to compare with those obtained from field measurements. Figure 5 shows the total deformation of the existing tunnel from starting the excavation of the deep foundation pit to completing the excavation work, in which the elastic model is used for simulating the segments of the shield tunnel structure, and the connections of the contact surfaces are treated with hard contact. The numerically calculated deformation of the existing tunnel is mainly distributed around the area adjacent to the deep foundation pit, the calculated and field measured maximum tunnel deformations are 0.74 mm and 0.7 mm, respectively, and there is an error of 5.26% between the numerically calculated and field-measured results. This can reflect the feasibility and accuracy of the adopted three-dimensional numerical model.

Figure 6 compares the calculated and field-measured ground settlements of the monitoring point around the deep foundation pit, in which the field monitoring point is marked as monitoring point M in the numerical model as shown in Figure 4, and the numerically calculated values of the monitoring point are fitted using spline curves. The field-monitored ground surface experienced nonlinear settlement with the gradually increased excavation depth of the deep foundation pit, in which the initial excavation to 5 m depth of the deep foundation pit resulted in the most increase in settlement, with significant disturbance to the soil surrounding the deep foundation pit. It can be clearly seen that the numerically calculated values of the monitoring point around the foundation pit are larger than those obtained from field measurement, and the results calculated by the constitutive model used in the simulation are more conservative, whereas the fitted curve of the calculated value is smooth and has a similar trend to the field-measured settlement curve of the monitoring point, which can reflect the surface subsidence law of the monitoring point in the practical engineering. Moreover, Figure 7 demonstrates the calculated and field-measured strain variation of the underground continuous wall during excavation. The calculated and field-measured maximum strains of the underground continuous wall are 160.9 με and 173.8 με, respectively, with an error of 7.4% between the numerically calculated and field-measured results. This also confirms the feasibility and accuracy of the adopted three-dimensional numerical model.

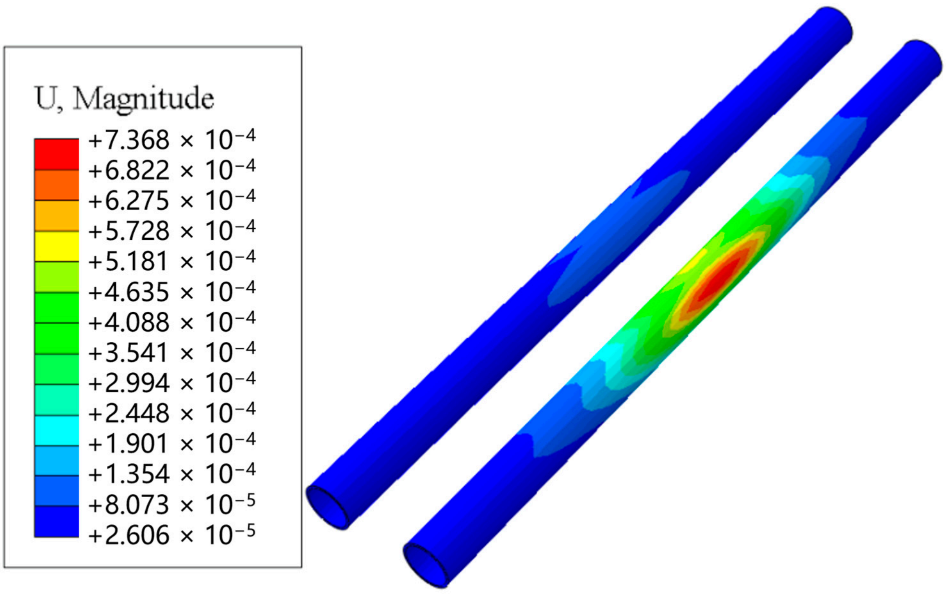

Figure 5. Tunnel deformation after excavating the bottom of the deep foundation pit (unit: m).

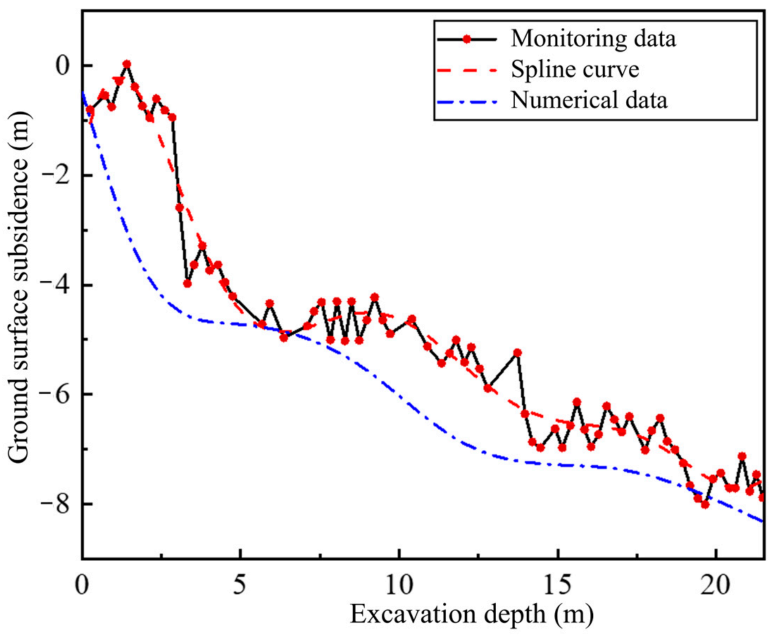

Figure 6. Calculated and field-measured ground settlements of the monitoring point.

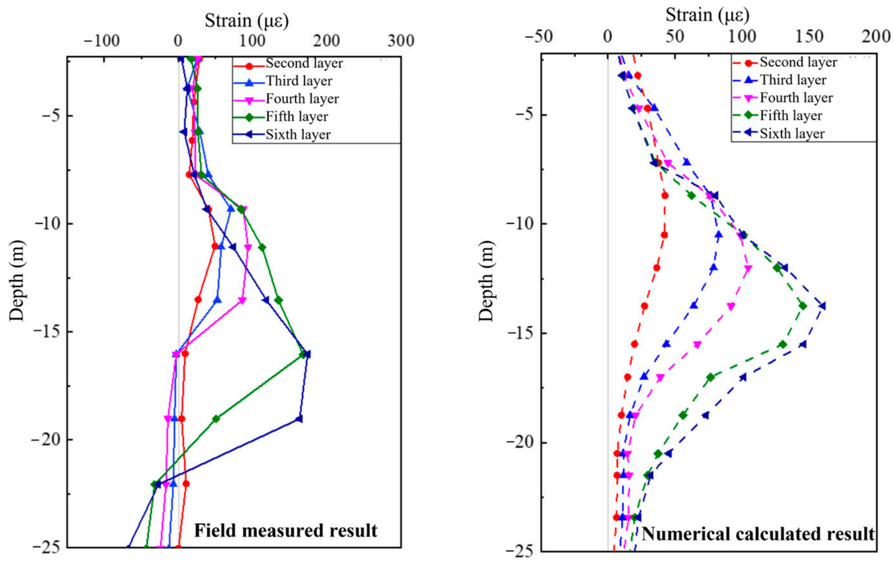

Figure 7. Calculated and field-measured strain variation of underground continuous wall during the excavation of the deep foundation pit.

4. Numerical Behavior Discussion of the Existing Tunnel Influenced by Excavating Adjacent Foundation Pit

4.1. Stress Analysis of Underground Continuous Wall

Figure 8 shows the stress distribution of the underground continuous wall during construction of the deep foundation pit. After completing the enclosure structure, small tensile stresses appeared at the corners of the underground continuous wall near the existing tunnel structure, whereas the other parts of the underground continuous walls were subjected to the compressive stresses under the constraint of the surrounding rocks, in which the stress state of the underground continuous wall showed tension on the inner side and compression on the outer side with the excavation of the deep foundation pit. The dominant stresses were located at the centerline of the underground continuous wall and decreased along the shape of the radiation circle, the maximum principal stresses were positioned on the west and south of the underground continuous wall, and the north connection of the underground continuous wall continued to decrease until the excavation depth of the deep foundation pit reached the fifth layer. The maximum principal stress on the underground continuous wall stabilized at the excavation depth of 13.75 m. When excavating to the bottom of the deep foundation pit, the position of the maximum principal stress on the underground continuous wall remained unchanged, and the maximum principal stress value decreased compared to the excavation of the fifth layer due to the good lithology of the soil surrounding the deep foundation pit. The maximum values of the principal stress appeared at the corner of the underground continuous wall during the excavation processes of the deep foundation pit, which can easily cause the corner concrete of the underground continuous wall to break and crack, leading to water seepage and damage in the enclosure structure of the deep foundation pit. This implies that it is reasonable to reinforce the corner of the adjacent tunnel structure.

4.2. Tunnel Structure Deformation

Figure 9 shows the deformation distribution of the existing tunnel structure during the construction stages of the deep foundation pit. It can be clearly seen that the dominant deformations of the existing tunnel structure occurred along the normal direction of the tunnel segment surface during the excavation of the deep foundation pit, in which the maximum deformation of the existing double-track tunnel structures was 0.7 mm, which is less than the control value of 10 mm. The deformation of the left-line tunnel structure is significantly greater than that of the right-line tunnel structure, and the maximum deformation of the tunnel structure is increased within the unchanged position during the excavation process of the deep foundation pit.

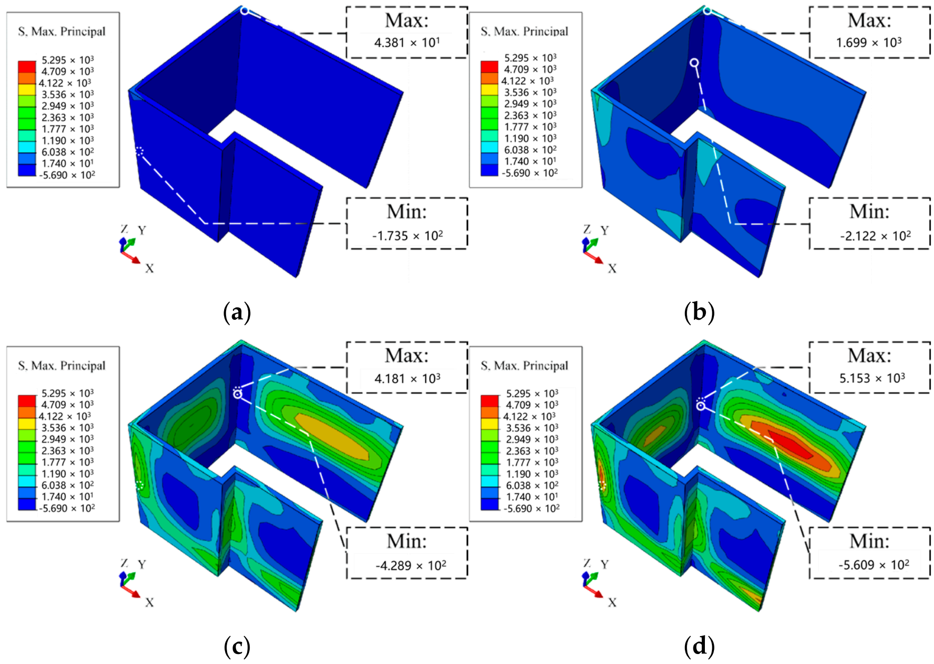

Figure 8. Stress in underground continuous wall during the construction process (unit: kPa). (**a**) After building continuous wall; (**b**) After excavating first layer; (**c**) After excavating third layer; (**d**) After excavating bottom of foundation pit.

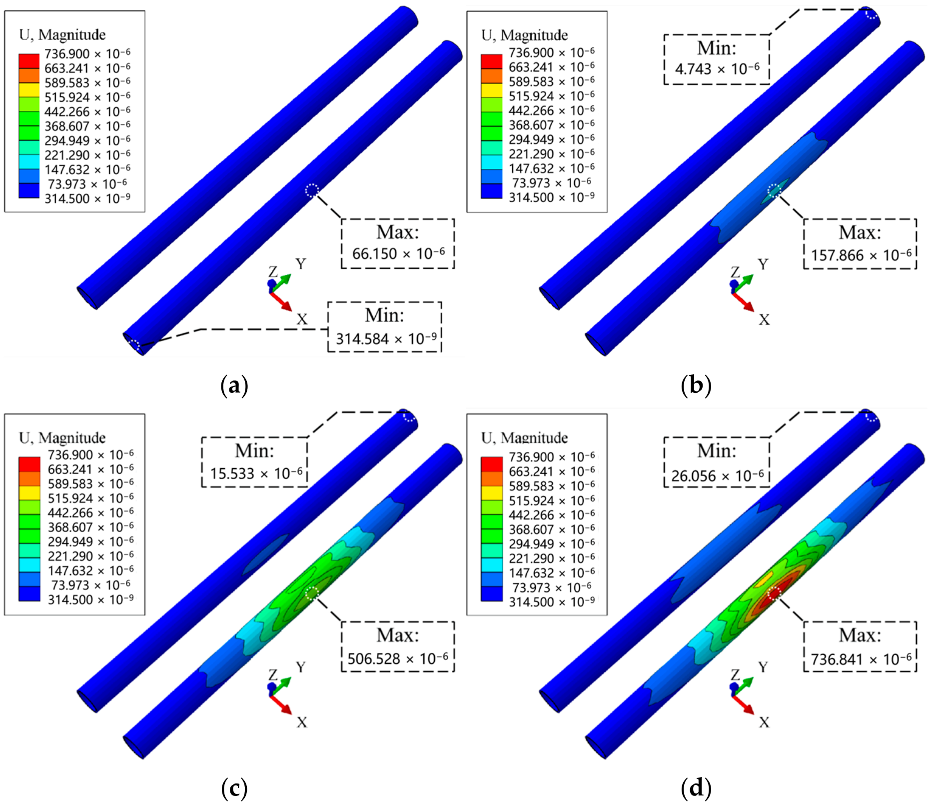

Figure 9. Tunnel deformation during the construction stages of excavating foundation pit (unit: m). (**a**) After building continuous wall; (**b**) After excavating first layer; (**c**) After excavating third layer; (**d**) After excavating pit bottom.

As demonstrated in Figure 9, the deep foundation pit is located in the significant influence area of the left-line tunnel structure belonging to existing rail transit line 7, at the shortest distance between the deep foundation pit and the existing double-track tunnel structures. The excavation of the deep foundation pit created less disturbance to the right-line tunnel structure belonging to the existing rail transit line 7. The deformation of the existing left-line tunnel structure reached its maximum value and gradually decreased outward starting from excavating the first layer of the deep foundation pit, and the deformation of the left-line tunnel structure was not symmetrical along the central axis, in which the deformation of the tunnel segment near the deep foundation pit was greater than the deformation of the tunnel segment on the other side. The increase in tunnel deformation caused by excavating the first, second and third layers of the deep foundation pit was greater than that caused by excavating the following three layers of the deep foundation pit.

Figure 10 shows the horizontal deformation of the left-line tunnel structure during the construction stages of excavating the deep foundation pit, in which the red area in the middle of the circle corresponds to the area seriously affected by the excavation. From the construction of the underground continuous wall to excavating the bottom of the deep foundation pit, the lateral displacement of the upper part of the left-line tunnel structure around the excavation side of the deep foundation pit was significantly greater than that of the lower part due to stress unloading in the left-line tunnel structure. The left-line tunnel structure is not in a uniform geological environment and the lower part of the left-line tunnel structure is constrained by medium to slightly weathered granite layers with good lithology, resulting in relatively small lateral displacement. Moreover, the maximum lateral deformation of the left-line tunnel structure is always located in a 45° clockwise deviation of the central axis of the tunnel structure, which has a maximum deformation value of 0.7 mm and an increase of 8.83 times, compared to building the underground continuous wall. Moreover, the increases in lateral deformation of the left-line tunnel structure during excavating the first, second and third layers are significantly greater than that of the excavation of the following three layers. The maximum lateral deformation of the right-line tunnel structure far from the deep foundation pit has an increase of 8.87 times compared to build the underground continuous wall, whereas the maximum lateral deformation is only 0.1 mm until excavating the bottom of the deep foundation pit. The maximum lateral deformation of the right-line tunnel structure is significantly less than that of the left-line tunnel structure near the deep foundation pit.

Figure 11 shows the vertical deformation of the left-line tunnel structure during the construction stages of excavating the deep foundation pit. The left-line tunnel structure has the most vertical deformation on the side near the deep foundation pit during the excavation, and the excavation of the deep foundation pit caused the side of the existing left-line tunnel structure to deform laterally and upwards. Moreover, the maximum positive vertical deformation of the left-line tunnel structure near the deep foundation pit is located at the arch foot of the tunnel structure during the excavation of the first and second layers, and that is always located at the center axis of the tunnel structure with a 45° clockwise deflection during the subsequent construction stages, in which the maximum positive vertical deformation is 0.35 mm with an increase of 73.48 times compared to build the underground continuous wall. The maximum negative vertical deformation of the left-line tunnel structure near the deep foundation pit is always located at the center axis of the tunnel structure with a 15° counterclockwise deflection, in which the maximum negative vertical deformation is 0.12 mm with an increase of 2.62 times compared to building the underground continuous wall. The maximum vertical deformation of the right-line tunnel structure far away from the deep foundation pit was significantly less than that of the left-line tunnel structure close to the deep foundation pit by an order of magnitude, which implies that the deformations of the existing tunnel structure were induced by the excavation of the deep foundation pit.

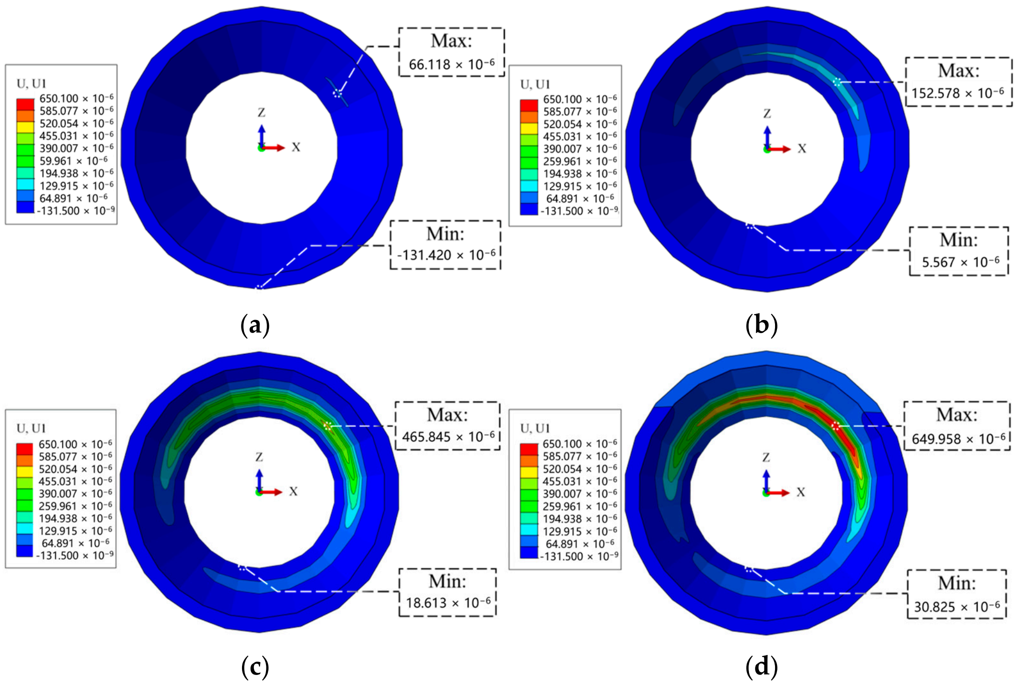

Figure 10. Tunnel deformation during various construction stages of excavating deep foundation pit (unit: m). (**a**) After building underground continuous wall; (**b**) After excavating first layer; (**c**) After excavating third layer; (**d**) After excavating bottom of foundation pit.

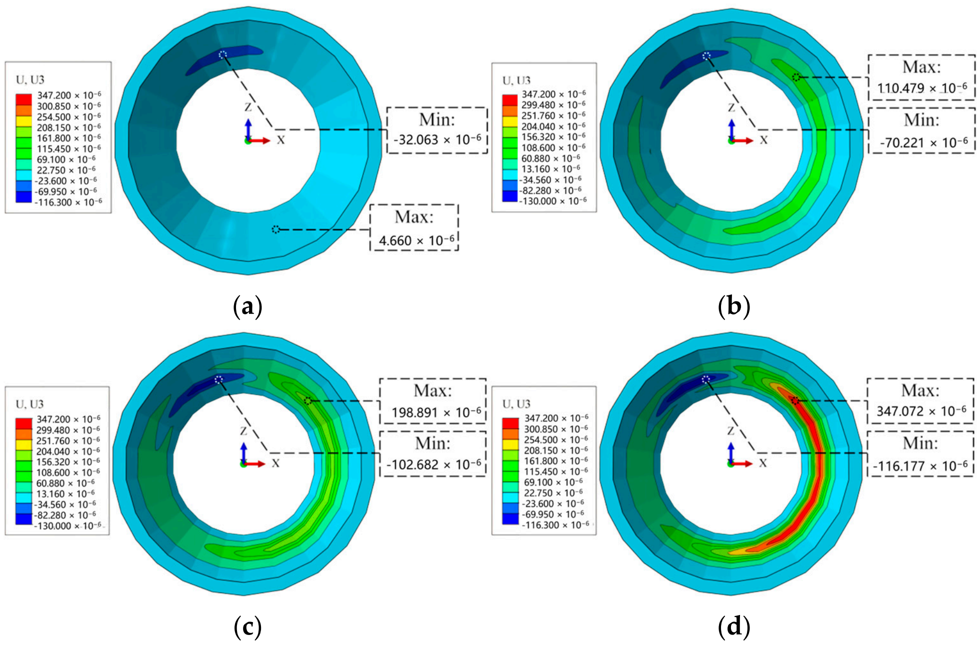

Figure 11. Vertical deformation of the left-line shield tunnel during each construction stage of excavating foundation pit (unit: m). (**a**) After building continuous wall; (**b**) After excavating second layer; (**c**) After excavating third layer; (**d**) After excavating pit bottom.

5. Conclusions

In this paper, the behavior of an existing underground rail transit line during excavating an adjacent deep foundation pit is numerically investigated in consideration of the very small distance between the deep foundation pit and the existing tunnel structure by employing a three-dimensional model. In the numerical analysis, the behavior of the existing tunnel structure from excavating the aforementioned foundation pit is studied, and the following conclusions can be drawn:

(1) The three-dimensional numerical model used is effective for evaluating the practical performance variation of the existing tunnel structure during excavating the adjacent deep foundation pit, with an error of 5.26% between the numerically calculated and field-measured maximum tunnel deformations of the existing tunnel structure. The numerically calculated settlement curve of the monitoring around the foundation pit is smooth and has a similar trend to the field-measured settlement curve of the monitoring point.

(2) The deep foundation pit is located in the significant influence area of the left-line tunnel structure belonging to existing rail transit line 7, in which the field-monitored ground surface experiences the nonlinear settlement with the gradually increased excavation depth of the deep foundation pit. The initial excavation to 5 m depth of the deep foundation pit resulted in the greatest increase in settlement with significant disturbance to the surrounding soil. Moreover, the excavation of the deep foundation pit created less disturbance to the right-line tunnel structure belonging to the existing rail transit line 7.

(3) The deformation of the left-line tunnel structure was significantly greater than that of the right-line tunnel structure, and the maximum deformation of the tunnel structure increased within the unchanged position during the excavation process of the deep foundation pit, whereas the horizontal and vertical displacements of the tunnel structure are within the range of the required control values, and the tunnel structure was safe during the excavation of the foundation pit.

(4) The left-line tunnel structure had the greatest vertical deformation on the side near the deep foundation pit during the excavation of the deep foundation pit, and the maximum lateral deformation of the right-line tunnel structure was significantly less than that of the left-line tunnel structure near the deep foundation pit, which implies that the excavation of the deep foundation pit caused the side of the existing left-line tunnel structure to deform laterally and upwards, and the deformations of the existing tunnel structure were more induced by the excavation of the deep foundation pit. Moreover, the increase in lateral deformation of the left-line tunnel structure during excavating the first, second and third layers was significantly greater than that of the excavation of the thereafter layers.

Author Contributions: Conceptualization, J.L., B.X., X.Z. and Y.Z.; validation, J.L. and H.W.; investigation, J.L. and B.X.; data curation, J.L.; writing—original draft preparation, J.L.; writing—review and editing, H.W. and Y.Z.; supervision, Y.Z.; funding acquisition, Y.Z. All authors have read and agreed to the published version of the manuscript.

Funding: This research was funded by Natural Science Foundation of Jiangsu Province (No. BK20211281), Six Talent Peak Projects.

Institutional Review Board Statement: Not applicable.

Informed Consent Statement: Not applicable.

Data Availability Statement: The data used to support the findings of this study are available from the corresponding author upon request.

Conflicts of Interest: The authors declare that there are no conflict of interest regarding the publication of this paper.

References

1. Wang, J.; Wang, P.C.; Wang, W.D.; Zhou, S.Q.; Fang, X. Optimization analysis of deformation of underlying tunnel in dewatering and excavation of phreatic aquifer. *Adv. Mater. Sci. Eng.* **2019**, *2019*, 2461817. [CrossRef]
2. Nguyen, B.P.; Ngo, C.P.; Tran, T.D.; Bui, X.C.; Doan, N.P. Finite element analysis of deformation behavior of deep excavation retained by diagram wall in Ho Chi Minh city. *Indian Geotech. J.* **2022**, *52*, 989–999. [CrossRef]
3. Wang, W.; Han, Z.; Deng, J.; Zhang, X.Y.; Zhang, Y.F. Study on soil reinforcement param in deep foundation pit of marshland metro station. *Heliyon* **2019**, *5*, e2836. [CrossRef]
4. Sazid, M.; Ahmed, H.A. Stability analysis of shallow depth tunnel in weak rock mass: 3D numerical modeling approach. *J. City Dev.* **2019**, *1*, 18–22.

5. Sun, H.S.; Chen, Y.D.; Zhang, J.H.; Kuang, T.S. Analytical investigation of tunnel deformation caused by circular foundation pit excavation. *Comput. Geotech.* **2019**, *106*, 193–198. [CrossRef]
6. Li, D. Superior research for selection of bracing structure of deep pit foundation based on fussy theory. In *Advanced Materials Research*; Trans Tech Publications Ltd.: Aedermannsdorf, Switzerland, 2013; pp. 838–841.
7. Chang, C.T.; Wang, M.J. Repair of displaced shield tunnel of the taipei rapid transit system. *Tunn. Undergr. Space Technol.* **2001**, *16*, 163–173. [CrossRef]
8. Zhang, Z.G.; Zhang, M.X.; Zhao, Q.H. A simplified analysis for deformation behavior of buried pipelines considering disturbance effects of underground excavation in soft clays. *Arab. J. Geosci.* **2015**, *8*, 7771–7785. [CrossRef]
9. Liang, R.Z.; Wu, W.B.; Yu, F.; Jiang, G.S.; Liu, J.W. Simplified method for evaluating shield tunnel deformation due to adjacent excavation. *Tunn. Undergr. Space Technol.* **2018**, *71*, 94–105. [CrossRef]
10. Zhang, X.M.; Ou, X.F.; Yang, J.S.; Fu, J.Y. Deformation response of an existing tunnel to upper excavation of foundation pit and associated dewatering. *Int. J. Geomech.* **2017**, *17*, 04016112. [CrossRef]
11. Zhang, X.H.; Wei, G.; Jiang, C.W. The study for longitudinal deformation of adjacent shield tunnel due to foundation pit excavation with consideration of the retaining structure deformation. *Symmetry* **2020**, *12*, 2103. [CrossRef]
12. Ye, S.H.; Zhao, Z.F.; Wang, D.Q. Deformation analysis and safety assessment of existing metro tunnels affected by excavation of a foundation pit. *Undergr. Space* **2021**, *6*, 421–431. [CrossRef]
13. Fan, S.Y.; Song, Z.P.; Xu, T.; Wang, K.M.; Zhang, Y.W. Tunnel deformation and stress response under the bilateral foundation pit construction: A case study. *Arch. Civ. Mech. Eng.* **2021**, *21*, 109. [CrossRef]
14. Yang, W.L.; Hu, Y.; Hu, C.; Yang, M. An agent-based simulation of deep foundation pit emergency evacuation modeling in the presence of collapse disaster. *Symmetry* **2018**, *10*, 581. [CrossRef]
15. Zhang, X.S.; Zhang, X.C.; Han, Y.S. A case study on field monitoring analysis of deep foundation pit in soft soils. *Adv. Civ. Eng.* **2019**, *2019*, 9342341. [CrossRef]
16. Wang, J.X.; Feng, B.; Yu, H.P.; Guo, T.P.; Yang, G.Y.; Tang, J.W. Numerical study of dewatering in a large deep foundation pit. *Environ. Earth Sci.* **2013**, *69*, 863–872. [CrossRef]
17. Lu, R.L.; Jiang, Q.H. Reinforcement scheme and numerical simulation for sequential excavation of the deep foundation pit. In *Applied Mechanics and Materials*; Trans Tech Publications Ltd.: Aedermannsdorf, Switzerland, 2012; Volume 1975, pp. 204–208.
18. Zhou, N.Q.; Vermeer, P.A. Numerical simulation of deep foundation pit dewatering and optimization of controlling land subsidence. *Eng. Geol.* **2010**, *114*, 251–260. [CrossRef]
19. Liu, H.F.; Li, K.Z.; Wang, J.Q.; Cheng, C. Numerical simulation of deep foundation pit construction under complex site conditions. *Adv. Civ. Eng.* **2021**, *2021*, 6669466. [CrossRef]
20. Sun, H.S.; Sun, W.B. Effect of soil reinforcement on tunnel deformation as a result of stress relief. *Appl. Sci.* **2019**, *9*, 1420. [CrossRef]
21. Tan, Y.; Huang, R.; Kang, Z.; Wei, B. Covered semi-top-down excavation of subway station surrounded by closely spaced buildings in downtown Shanghai: Building response. *J. Perform. Constr. Facil.* **2016**, *30*, 04016040. [CrossRef]
22. Zhang, Y.X.; Yang, J.S.; Yang, F. Field investigation and numerical analysis of landslide induced by tunneling. *Eng. Fail. Anal.* **2015**, *47*, 25–33. [CrossRef]